Hybrid lipid-nanoparticle complexes for biomedical applications

Kevin M. Vargas and **Young-Seok Shon**

Department of Chemistry & Biochemistry, California State University Long Beach, Long Beach, California 90840-9507, USA.

Abstract

Biomolecule-nanoparticle hybrids have proven to be one of most promising frontiers in biomedical research. In recent years, there has been an increased focus on the development of hybrid lipid-nanoparticle complexes (HLNCs) which inherit unique properties of both the inorganic nanoparticles and the lipid assemblies (i.e. liposomes, lipoproteins, solid lipid nanoparticles, and nanoemulsions) that comprise them. In combination of their component parts, HLNCs also gain new functionalities which are utilized for numerous biomedical applications (i.e. stimuli-triggered drug release, photothermal therapy, and bioimaging). The localization of nanoparticles within the lipid assemblies largely dictates the attributes and functionalities of the hybrid complexes and are classified as such: (i) liposomes with surface-bound nanoparticles, (ii) liposomes with bilayer-embedded nanoparticles, (iii) liposomes with core-encapsulated nanoparticles, (iv) lipid assemblies with hydrophobic core-encapsulated nanoparticles, and (v) lipid bilayer-coated nanoparticles. Herein, we review the properties of each hybrid and the rational design of HLNCs for biomedical applications as reported by recent investigations. Future directions in advancing and expanding the scope of HLNCs are also proposed.

Graphical Abstract

This paper reviews five different types of hybrid lipid-nanoparticle complexes (HLNC) with potential applications in biomedical research.

1. Introduction

With the continued advancements in the emerging field of nanotechnology, its implications in biomedicine have also expanded. Researchers have increasingly utilized nanomaterials and their unique properties for numerous biomedical applications.[1–4] Gold nanoparticles (AuNPs) are most prominently used because of their low acute toxicity, easily modulated surface chemistry, tunable size and shape parameters, as well as their incredibly valuable optical and electronic properties.[1] Most notably, the strong localized surface plasmon resonance (LSPR) of AuNPs has been implemented in a variety of ways including bioimaging, drug delivery and photothermal cancer therapy.[1] Other noble metal nanoparticles such as silver and palladium nanoparticles (AgNPs and PdNPs) have also found specialized roles; AgNPs are known anti-microbial and anti-inflammatory agents,

Conflicts of interest
There are no conflicts to declare.

while the robust catalytic activity of PdNPs warrants its potential applications in prodrug activation and as enzyme site mimics.[5–7] The biocompatibility and distinct magnetic properties of super paramagnetic iron oxide particles (SPIONs) make them model MRI contrast agents and are also utilized in magnetic fieldguided drug delivery systems.[8] Additionally, semiconducting nanoparticles called quantum dots (QDs) are often used as optical probes in bioimaging over traditional organic dyes due to their great chemical degradation and photobleaching resistance, large extinction coefficient, and general size-dependent optical properties.[8–10]

Much research is focused on the development of biomolecule-nanoparticle hybrids, which not only retains the inherent properties of each of its component parts, but also in combination, inherits new functionality.[10] Many hybrids of the aforementioned inorganic nanoparticles and biomolecules (i.e. nucleic acids, proteins, peptides, carbohydrates, or lipids) have been developed with proposed applications in cellular labelling, bioimaging, gene therapy, drug delivery, and biocatalysis, among others.[11–17] Herein, we focus on hybrids of inorganic nanoparticles and lipid assemblies (i.e. liposomes, lipoproteins, solid lipid nanoparticles, and nanoemulsions), appropriately termed as hybrid lipid-nanoparticle complexes (HLNCs).

Liposomes have long served as *in vivo* carrier systems for drug delivery notably capable of entrapping drug molecules and improving overall bioavailability and activity.[18] Liposome-based pharmaceutical products have already had much clinical successes, with the prime example being Doxil®, an anti-cancer drug approved by the US Food and Drug Administration (FDA).[21] The multifaceted clinical applicability of liposomes is rooted in some of its key attributes, which sequentially make them desirable biomolecule components in hybrids with nanoparticles. The capacities to be bound by particles at the liposomal surface through interactions with the zwitterionic phospholipid head groups, to integrate lipophilic components within the bilayer, and to encapsulate hydrophilic components within the aqueous core are all valuable in designing HLNCs with directed localization of nanoparticles for specified functionalities. Additionally, a large selection of phospholipids can be used to formulate liposomes with regulated physicochemical properties such as size, permeability, surface charge, and gel-liquid phase transition temperatures (Tc). Furthermore, the surface of liposomes can be modified with various structural components to promote increased stability, targeting mechanisms, and labelling capabilities. Each of these attributes contributes to the design of HLNCs with desired functionalities.

Similarly, lipoproteins, solid lipid nanoparticles (SLNs), and nanoemulsions can encapsulate particles within their hydrophobic cores, offering their own advantages as host biomolecules. Lipoprotein hybrids are primarily targeted towards the uptake into cells with an overexpression of LDL (low-density lipoprotein) receptors such as tumour cells. SLNs, composed of a solid lipid core stabilized by surfactant molecules, serve as an alternative lipid-based delivery platform to liposomes. Nanoemulsions addressed in this review are dispersions of perfluorocarbons in water, stabilized by phospholipid surfactants.

For the purposes of this review, HLNCs are categorized into five types based on the localization of the nanoparticles within the lipid assembly: (i) liposomes with surface-bound

nanoparticles, (ii) liposomes with bilayer-embedded nanoparticles, (iii) liposomes with core-encapsulated nanoparticles, (iv) lipid assemblies with hydrophobic core-encapsulated nanoparticles, and (v) lipid bilayer-coated nanoparticles (Fig. 1). Herein, we review the properties of each hybrid and the rational design of HLNCs for biomedical applications.

2. Liposomes with surface-bound nanoparticles

2.1 Nanoparticle-induced stabilization of liposomes against fusion

A limitation of liposomes for biomedical applications, especially for those smaller than 100 nm in diameter, is their tendency to fuse with each other to form larger vesicles.[22–24] For certain applications, such as dermal drug delivery, the increased liposome size may restrict the carriers' transport capabilities.[25–26] Many other issues arise from liposome fusion including the increased size dispersity, transient leakage of encapsulated contents during the act of fusion, and unintended mixing of contents.[27] A popular approach for stabilizing liposomes against fusion is to cover the liposomal surfaces with a protective coating, most notably with poly(ethylene glycol) (PEG).[28] Although effective in intent, the protective PEG coating greatly limits interactions of the liposomal surface. An alternate strategy is stabilization via surface-bound nanoparticles. In 2006, Zhang and Granick first employed this strategy by simple mixing of negatively charged carboxyl-modified polystyrene (PS) nanoparticles and DLPC liposomes doped with fluorescent label DMPE-RhB.[27] The charged nanoparticles adsorb to the zwitterionic head groups of surface lipids through charge-dipole and non-specific interactions. Fusion is prevented by electrostatic repulsion and steric between the surface-bound nanoparticles of encroaching liposomes. The resulting HLNC is found to be stable against fusion at high volume fractions of the hybrid and even after prolonged periods of time, as monitored via the translation diffusion coefficient. Furthermore, the surface-bound nanoparticles occupy only 25% of the surface preserving the potential for surface interactions. Additional studies confirmed the accessibility of the unoccupied surface for interactions such as protein binding in the presence of stabilizing nanoparticles.[29] More recently, AuNPs with charged passivating ligands or surfactants, have emerged as a favoured stabilizing nanoparticle.[30]

For certain delivery applications, controlled fusion can be used to release or transport liposomal contents at specific target sites. Stimuli-triggered detachment of stabilizing nanoparticles is a strategy to accomplish this goal. For example, AuNPs coated with mercaptopropionic acid (MPA) ligands adsorb via electrostatic interactions onto the surface of liposomes with cationic DOTAP phospholipids at neutral pH, at which the negatively charged deprotonated carboxylate form of the ligands dominates.[31] Upon exposure to acidic conditions, the carboxylate moieties are protonated, triggering the detachment of AuNPs and leaving liposomes vulnerable to fusion. For drug delivery target sites residing in acidic environments, such as at skin lesions, this type of HLNC may be valuable. Conversely, liposomes partially composed of anionic DOPA phospholipid are stabilized by cationic chitosan-coated AuNPs that remain adsorbed at acidic conditions and detach at neutral conditions. In this case, the phospholipid DOPA is the pH sensitive component and loses its negative charge at physiological pH of 7.4.[32] This type of HLNC has a potential for treatment of infections in the mucus lining of stomach, where pH approaches neutral

conditions. Thamphiwatana et al. confirmed the pH-dependent bacterial membrane fusion and drug-release capabilities of the aforementioned HLNC, using *H. pylori* bacteria and model drug doxycycline.[32] The doxycycline-loaded HLNC exhibits augmented antibacterial effects compared to that of free doxycycline, which is thought to be due to the high efficiency of delivering drugs to bacteria via the fusion process (Fig. 2).

2.2 Nanoparticle-induced phase transition of lipid membrane

Greater understanding of the interactions between nanoparticles and the surface of liposomes allows better control in designing HLNCs with intended physicochemical properties. Alternately, liposomes with surface-bound nanoparticles can be used as a model to study the effects of nanoparticles on biological membranes, which is especially relevant with the extensive integration of AuNPs in biomedical applications.

A central property of lipid membranes is its fluidity or phase behaviour. At its gel-liquid phase transition temperature (T_c), the lipids transition from a low fluidity gel-phase to a high fluidity liquid-phase. As observed by Wang et al., upon binding of negatively charged PS nanoparticles onto liposomes composed of either DOPC ($T_c = -20$ °C) or DLPC ($T_c = -1$ °C) at room temperature, lipids interacting with nanoparticles experienced local gelation. [33] This phase change is a result of the outward shift in the orientation of the zwitterionic head groups of lipids allowing the interaction with the nanoparticles and subsequently inducing increased packing density as shown in Fig. 3. For the similar reasons, positively charged PS nanoparticles induce local fluidization of liposomes composed of gel-phase DPPC ($T_c = +40$ °C), although to a lesser extent due the weaker binding interactions of cationic nanoparticles. It is concluded that the rigidly directed charge of the nanoparticles plays a role in inducing the phase-transition, as more flexible charged species (i.e. DNA) are unable to reproduce these outcomes. When citrate-capped AuNPs adsorb onto liquid-phase DOPC and DMPC ($T_c = +23$ °C) liposomes, nanoparticle aggregates form. However, this is not observed to a significant extent in binding gel-phase DPPC.[34] Wang et al. proposed that upon nanoparticle-induced local gelation of DOPC and DMPC liposomes, it is thermodynamically favoured for gel-phase regions to merge and minimize liquid/gel interfaces, resulting in nanoparticle aggregation. In comparison, MPA-AuNPs exhibit limited aggregations on DOPC and DMPC liposomes. Conclusions can be made that the interactions between nanoparticles and lipids are a combination of electrostatic and van der Waals attractions. Citrate is an easily displaced ligand, allowing AuNP core to interact more intimately with the lipid than the core of MPA-AuNP. Stronger nanoparticle-lipid interactions induce a greater extent of induced phase-transition, leading to nanoparticle aggregate formation in liquid-phase liposomes. These are important considerations in designing HLNCs of this type.

In addition, laurdan probe assays with citrate-capped AuNP adsorbing onto the surface of DMPC liposomes reveal that local gelation induces long-range fluidization of unbound lipids of the liposomes.[35] The shape of the liposomes are distorted as a result of the overall fluidization and in some cases membrane pores are formed. Furthermore, during nanoparticle-induced phase transition the packing of lipids undergoes great fluctuation between gel and liquid-phase. The perturbation of the membrane during the transition allows

the transient leakage of liposomes.[36] Using encapsulated fluorescent calcein probes, Wang and Liu observed this transient leakage during both adsorption and desorption of citrate-capped AuNP onto fluid-phase liposomes composed of either DOPC or DLPC, however not with gel-phase liposome composed of DPPC. MPA-AuNPs adsorbed to liposomes show no signs of transient leakage. Surface adsorption of CeO_2 nanoparticles (nanoceria) causes transient leakage in DOPC liposomes but not DPPC liposomes.[37] The ability to release liposomal content upon adsorption and desorption of nanoparticles has potential uses in triggered-release applications.

2.3   Biomedical applications of type (i) HLNCs

In recent years, liposomes with surface-bound nanoparticles have been developed for applications in stimuli-triggered drug release, photothermal therapy (PTT), DNA sensing/transfection, and biolabelling. These functionalities are engineered through modulation of all parameters of the HLNC including nanoparticle surface coatings, lipid compositions, liposomal membrane contents, surface modifications, and so forth.

For drug delivery systems, a valued mechanism is the controlled release of contents at specific target sites. A common strategy is the design of carriers with stimuli-triggered release, either with internal (i.e. pH, presence of toxins, or enzymatic activity) or external stimuli (i.e. light or magnetic field). Previously discussed was a HLNC designed to detach nanoparticles in acidic environments for dermal drug delivery, in which the charge of the nanoparticle coating is the stimuli-sensitive component. Modifications to the liposomal membrane can also elicit triggered-drug release capabilities. An interesting case is with chitosan-AuNP stabilized EPC liposomes designed to have an enhanced sensitivity to bacterial toxin pore formation by controlling the cholesterol content within liposome membranes and the extent of PEGylation.[30] In the presence of toxin-secreting bacteria, such as methicillin-resistant *Staphylococcus aureus* (MRSA), toxins form pores in the membranes of the HLNC and loaded antibiotics, such as vancomycin, are released locally. Another manner of evoking triggered-drug release is through incorporating stimuli-sensitive phospholipids into the liposome formulation. DSPG phospholipids are especially prone to phospholipase A2 (PLA2)-mediated degradation. Accordingly, in an effort to target PLA2-secreting bacteria such as *H. pylori*, DSPG phospholipids are incorporated into chitosan-AuNP stabilized liposomes by Thamphiwatana et al.[38] In the presence of *H. pylori*, secreted PLA2 enzyme degrades membrane DSPG to release model drug doxycycline and effectively inhibit bacterial activity (Fig. 4). For light-triggered release mechanisms, gold nanoshells and other gold nanostructure morphologies are commonly used as the stimuli-sensitive component. Nanoshells can be tuned to have LSPR at near-infrared (NIR) wavelengths, which is desirable in biomedical applications due to the relatively deep penetration of NIR radiation into soft tissue. A common strategy is to use liposomes as soft templates for biodegradable nanoshell formation.[39–41] Exposure to NIR radiation causes these gold nanoshells to dissipate heat resulting in a gel to fluid phase transition of otherwise gel-phase liposomes (i.e. DPPC and DSPC) and subsequent drug release. Many times, these types of HLNCs are multifunctional and can also simultaneously be used for PTT; Rengan et al. successfully demonstrated PTT capabilities of this hybrid *in vitro* and *in vivo*.[40,42] Enzymatic degradation of the liposomal core allows nanoshell structure to collapse and

degrade into small AuNPs that can undergo renal clearance; alternatively, prolonged NIR irradiation also causes nanoshell degradation.[40–42]

HLNCs play a key role in novel DNA sensing and transfection methods. In one such method, citrate-AuNP stabilized DOTAP liposomes are first tethered to a gold transducer via a thiol monolayer. Thiolated single stranded DNA (ssDNA) are then fixed onto AuNPs. At this juncture, the complementary strand can be sensed at very low detection limits through hybridization with the AuNP-fixed ssDNA. Alternately, the HLNC can also be used for transfection of the ssDNA.[43–44]

3. Liposomes with bilayer-embedded nanoparticles

3.1   Effects of embedded nanoparticles on bilayer properties

In contrast to the nanoparticles incorporated in type (i) HLNCs, which are relatively large and charged (i.e. 20 nm citrate-capped AuNP), bilayer embedded nanoparticles are small and hydrophobic. The size and loading concentrations of embedded nanoparticles have been reported to affect the lipid packing, fluidity, gel-fluid phase transition temperature, and thickness of phospholipid bilayers.

The fluidity of liposome bilayers as a function of nanoparticle loading concentrations was investigated by Park et al., using 3–4 nm stearylamine-capped AgNPs embedded into the bilayers of DPPC liposomes.[45] Above the transition temperature of DPPC, at which it would exist in liquid phase, increasing nanoparticle loading concentrations results in increasing fluidity of the bilayer. However, the increase in fluidity is not observed below the transition temperature. The same results are also reported for the equivalent AuNPs confirming the insignificant influence of AuNP on the fluidity of DPPC bilayers below the transition temperature.[46] Dodecanethiol-capped AgNPs (5.7 ± 1.8 nm) embedded into the bilayers of DPPC liposomes, however, increase fluidity for both above and below the phase transition temperature.[47] This discrepancy elucidates that the larger particles disrupt the order of gel-phase bilayer to a greater extent than the smaller particles. Additionally, the dodecanethiol-capped AgNPs are shown to depress the transition temperature of DPPC with increasing nanoparticle loading concentrations. The ability to embed particles larger than the length of the bilayer is also displayed in the case of dodecanethiol-capped AgNPs. On the contrary, an increase in lipid order of DPPC bilayer is observed for oleic acid-capped maghemite SPIONs, exemplifying a stabilizing effect with embedding of nanoparticles.[48]

Preiss et al. investigated the effects of nanoparticle size on thermal leakage of DPPC liposomes using 2 and 4 nm dodecanethiol-capped AuNPs, with the 2 nm nanoparticle being smaller than the bilayer thickness and the 4 nm nanoparticle being close to bilayer thickness. The results indicated that the smaller nanoparticles reduce the thermal-induced permeability of the bilayer to a greater extent than the larger nanoparticles.[49]

The dispersion or clustering of nanoparticles within the bilayer is a phenomenon that has also been investigated. Through either coextrusion of EPC phospholipids and dodecanthiol-capped AuNPs (< 2 nm) or a dialysis method involving mixing pre-formed liposomes with nanoparticles dispersed in detergent, a dense AuNP monolayer or Janus clustering within the

bilayer are observed, respectively.[50] In this case the clustering is likely due to a combination of the small nanoparticle size, the liquid-phase bilayer, and the high nanoparticle loading concentrations. For stearylamine-capped AuNPs embedded into DPPC bilayers, the nanoparticles are observed to be dispersed in gel-phase but clustered in liquid-phase.[51] This is reasoned by greater hydrophobic mismatch in liquid-phase, a property that drives transmembrane protein aggregation.

3.2   Biomedical applications of type (ii) HLNCs

The intimate contact of nanoparticles with the bilayer in type (ii) HLNCs makes them especially effective in stimuli-triggered thermal release applications. Seclusion of nanoparticles within the bilayer allows for applications in which HLNC undergoes cellular internalization or fusion with target cell membrane.

Liposomes with bilayer-embedded SPIONs are often used for triggered-release mechanisms initiated by radio frequency alternating magnetic fields (AMFs). Upon exposure to AMFs, SPIONs generate heat locally resulting in increased permeability or rupture of the bilayer membrane and subsequent release of drugs or other therapeutic agents. AMF-triggered release of fluorescent dyes is demonstrated using 5 nm oleic acid-capped maghemite SPIONs embedded into DPPC liposome bilayers.[48] The same hybrid is further investigated for its ability to co-release hydrophobic raloxifene HCl (RAL) residing in bilayer and doxycycline HCl (DOX) residing in aqueous core of the liposomes.[52] Exposure to AMFs triggers the significant release of DOX, however, RAL release is limited due to its high affinity for the lipid bilayer. Amstad et al. aimed to improve the stability of these hybrids by PEGylating the liposomes and moving on from oleic acid-capped SPIONs in favour of palmityl-nitroDOPA-capped SPIONs that are less prone to aggregation and more easily integrated into liposome bilayers than oleic acid-capped SPIONs. [53]

Beyond simply initiating the release of drugs or therapeutic agents, nanoparticles can also contribute to enhanced therapeutic effectiveness. In an effort to combine the advantages of two drug delivery methods, namely via liposomal encapsulation or nanoparticle-conjugation, Bao et al. designed an intriguing bilayer-embedded HLNC (Fig. 5).[54] AuNPs are capped by PTX-PEG-SH ligands, a derivative to anti-cancer drug paclitaxel (PTX), and embedded in the bilayer of PC liposomes. This hybrid has shown a relatively high loading capacity, a prolonged release rate (50% of drug released over the span of 6 days), and an extended circulation time. The therapeutic efficacy of the hybrid for mice tumours is similar to control PTX. However, it is thought the prolonged release rate would result in greater effects over time. The efficacy of this delivery system is further enhanced by also loading both free PTX and PTX-PEGAuNPs into liposomes for both fast-release and sustained-release of PTX.[55] Another example of HLNC-enhanced therapeutics is with dodecanethiol-AuNPs loaded into HSPC liposomes containing Rose Bengal (RB), a photosensitizer used in photodynamic therapy.[56] The AuNPs of the HLNC are reported to enhance singlet oxygen generation by as high as 1.75 times that of solely RB loaded liposomes.

Controlled labelling of human embryo kidney cells (HEK293) using HLNCs was demonstrated by Gopalakrishnan et al. The localization of trioctylphosphineoxide-capped QDs (CdSe) in the bilayer of DMPC/DOTAP liposomes promotes unobstructed cellular

internalization for labelling of targets within the cell.[57] Upon doping the liposome formulation with PEG-conjugated lipids, the hybrid vesicle undergoes fusion with cellular membrane (Fig. 6). This mechanism is thought to be due to PEG acting as a barrier to internalization, keeping the liposomal and cellular membranes at a distance where membrane fusion is promoted.

4. Liposomes with core-encapsulated nanoparticles

4.1 Synthesis of metal nanoparticles within liposomal core

An emerging method for controlled metal nanoparticle synthesis is to react metal nanoparticle precursors and reducing agents within the aqueous core of liposomes. In one method, liposomes of various lipid formulations are quickly formed in a solution containing metal precursor and reducing agent, encapsulating both species within the aqueous core and eventually resulting in the formation of metal nanoparticles (Fig. 7).[58] Of particular interest is how the lipid composition affects the size distribution of prepared nanoparticles. Using liquid-phase DOPG, DOPE, or gel-phase DPPC liposomes with encapsulated glycerol reducing agent and palladium precursor, Clergeaud et al. prepared nanoparticles with sizes of **2.6 ± 0.7**, **9 ± 3**, and **16 ± 2** nm, respectively.[59] DOPG liposomes produce the smallest nanoparticles, which can be attributed to the contribution of DOPG's glycerol head group to the reduction of the palladium. The size discrepancy between nanoparticles prepared in liquid- and gelphase liposomes is due to the permeability of the bilayer membranes to the extra-liposomal glycerol. Ordered gel-phase DPPC bilayers restrain the flow of glycerol into the liposomal core, effectively limiting the reducing agent/palladium ratio, and resulting in larger particle size. Conversely, liquid-phase liposomes are more permeable and enable higher reducing agent/palladium ratios producing nanoparticles with smaller core sizes.

In another method, DSPC liposomes with aqueous core encapsulated reducing agents are preformed and dispersed in an aqueous solution of metal precursors (Au, Ag, Pd, and Pt) (Fig. 7).[60] The metal precursor diffuses into liposomal core where it is reduced, resulting in HLNC formation. Due to the fixed amount of reducing agent available within the liposomal core, combined with a large reservoir of metal precursor, a single nanoparticle occupying the entirety of each core is formed. This is advantageous in that the nanoparticle size can easily be tuned by using different sized liposomes in preparation. Lee et al. also demonstrated that bimetallic nanoparticles (Au/Pt, Au/Pd, and Au/Ag) can be synthesized by using mixed metal precursor solutions. The ability to control both the size and metal composition of nanoparticles allows tuning of LSPR more precisely. The prepared HLNCs have higher stability in physiological conditions and greater endocytosis efficiency than non-encapsulated gold nanoparticles, allowing for potential bioimaging applications.

4.2 Biomedical applications of type (iii) HLNCs

Similar to type (i) and type (ii) HLNCs, stimuli-triggered drug release through localized heating of liposomal bilayer is a proposed application of liposomes with encapsulated nanoparticles. Investigations of release capabilities of this type of HLNC have been conducted using light (visible or near-infrared) induced heating of encapsulated gold

nanoparticles (nanorods or nanostars) and AMF-induced heating of encapsulated SPIONs with success using fluorescent dyes.[61–63]

5. Lipid assemblies with hydrophobic core-encapsulated nanoparticles

5.1 Lipoprotein-based HLNCs

Highly proliferative tumours undergoing membrane biogenesis have a high demand for cholesterol, justifying the overexpression of LDL receptors in these cells. Lipoproteins, which serve a primary role in transporting lipids in the bloodstream, are often used as vehicles for targeting tumours. In an effort to target human brain glioblastoma cells, Chuang et al. encapsulated AuNPs within the hydrophobic core of reconstituted high-density lipoprotein (HDL).[64] Tetradecanethiol-capped AuNPs with diameters of 3, 10, or 17 nm are co-sonicated with DMPC and recombinant apolipoprotein E3 (apoE3) in PBS solution resulting in the formation of hybrids. Preparation of hybrids using 3 nm AuNPs leads to the formation of 60–80 nm lipoproteins with many encapsulated nanoparticles. When 10 and 17 nm AuNPs are used, it results in the formation of 22 and 28 nm lipoproteins, respectively, with each encapsulating a single nanoparticle in the core (Fig. 8). The surface plasmon bands of each HLNC around 520 nm confirm the stability of encapsulated AuNP against aggregation. LDL receptor binding assays suggest that LDL receptor binding sites and required conformation for receptor binding are preserved even in the presence of AuNPs. In *in vitro* uptake studies with human glioblastoma A172 cells, the AuNPs are found to be in the perinuclear region which provides evidence for LDL receptor-mediated endocytosis. In addition, internalized AuNPs are observed to be aggregated, allowing for potential applications in photothermal therapy.

LDL-based HLNCs with encapsulated AuNPs are also investigated for potential applications in biolabelling.[65] Dodecanethiol-capped AuNPs (2–3 nm) encapsulated by LDL results in HLNCs with around 20 nm in diameter, which is comparable to that of native LDL. Preserved receptor-mediated uptake is confirmed *in vitro* via competitive inhibition assays with various LDL receptor possessing cells and *in vivo* via an LDL receptor KO mice experiments. When the LDL-based HLNC is introduced to mice with B16-F10 tumours, most of the HLNCs are taken up by tumour-associated macrophages (TAMs). TAMs are previously shown to be correlated with metastasis of tumour cells, thus making it a potentially useful target for studying and treating cancer.[66]

5.2 Solid lipid nanoparticle-based HLNCs

As an alternative to liposomes, SLNs are one of the emerging lipid-based platforms for drug delivery. SLNs are composed of a solid lipid core, where drugs, therapeutic agents, and nanoparticles can be contained, stabilized by surfactant molecules. SPION-SLN hybrids have been prepared by Grillone et al. using SLNs made of cetyl palmitate and loaded with anti-cancer drug sorafenib for antitumor applications.[67] Within the core, the SPIONs form clusters yet retain their superparamagnetic properties. These HLNCs demonstrate the antiproliferative activity against human hepatocarcinoma HEPG2 and the ability to be magnetically directed towards accumulation at tumour sites. The SPION-SLN hybrids also

exhibit enhanced properties as MRI contrast agents compared to common SPION-based contrast agents.[68]

5.3   Nanoemulsion-based HLNCs

Nanoemulsions are dispersions of oil in aqueous phase stabilized by surfactants. Nanoemulsion-based HLNCs have been developed by Lim et al. using various perfluorocarbons and phospholipid surfactants with encapsulated QDs. The successful use of these hybrids as bimodal nanoprobes for differential imaging of therapeutic cells (macrophages, dendritic cells, and nonphagocytic T cells), which can be a useful monitoring tool in immune cell-based therapies, is demonstrated.[69] In constructing the HLNCs, the trioctylphosphineoxide (TOPO) ligands of the QDs (CdSe/ZnS) are exchanged with $1H,1H,2H,2H$-perfluorooctanethiol to allow better dispersion of QDs in the perfluorocarbon nanoemulsions. The strategy uses the ^{19}F-MR properties of perfluorocarbons and the fluorescent optical properties of QDs for differential imaging. The significant uptake of nanoemulsion hybrids into the therapeutic cells, with 90.55% for macrophages, 85.34% for dendritic cells, and 33% for T cells, are observed. An *in vivo* detection of labelled therapeutic cells injected into mice is also demonstrated using both MR and optical means of imaging. The uptake of these HLNCs in natural killer cells, which are typically difficult to label with imaging probes, is confirmed.[70] Labelling with the nanoemulsion-based hybrids shows no cytotoxic effects on the natural killer cells at the hybrid concentrations tested.

Detection of breast cancer cells is also accomplished through modification of the nanoemulsion hybrid.[71] An antibody-conjugated variation of the perfluorocarbon/QD nanoemulsions is constructed by including N-hydroxysuccinimide modified phospholipids (DSPEPEG$_{3400}$-NHS) in the surfactant formulation, which are able to link with the amine groups in antibodies. Various antibodies that target growth factors overexpressed in human breast cancer cells are conjugated onto the nanoemulsions. Each hybrid with a specific antibody is demonstrated to selectively bind to its target breast cancer cell line.

6.   Lipid bilayer-coated nanoparticles

6.1   Cationic lipid bilayer-coated nanoparticles

An early example of lipid bilayer-coated nanoparticles was prepared by reducing aqueous Au precursor in the presence of cationic lipid DDAB.[72] The DDAB passivates the gold nanoparticle core via interactions with positively charged ammonium groups and anchors the outer DDAB leaflet resulting in bilayer-coated AuNPs. Naturally, the positive surface charge of this HLNC led researchers to explore its interaction with DNA and its potential as a non-viral vector for transfection. When cationic lipid bilayers (either DDAB or DODAB) are coated onto AuNPs, the complex with DNA exhibits enhanced stability.[73–74] The transfection efficiency of plasmid DNA into HEK 293 cells are up to five times greater for DODAB bilayer-coated AuNPs compared to DODAB alone.[74] Cationic lipid bilayer-coated nanoparticles also show enhanced transfection efficiency when used in conjunction with cationic liposomes such as DOTAP.[75] This enhanced transfection is justified by the increased DNA packing density of the complex formed between the liposome, DNA, and HLNC allowing for more internalized DNA during transfection.

6.2   Alkanethiol-anchored bilayers

Another approach in preparing lipid bilayer-coated nanoparticles is to use nanoparticle-bound alkanethiols to anchor outer leaflet phospholipids via interactions between hydrophobic chains. This type of HLNC formation was first achieved when AuNPs are prepared by reduction of Au precursor in presence of phospholipids, which is followed by the addition of decanethiol. The produced AuNPs are found to be especially resistant to cyanide etching at high concentrations of KCN for prolonged periods of time.[76] This high resistance to etching is rationalized by the formation of a bilayer coating around the AuNP core that makes permeations more challenging for ions such as cyanide. When the higher concentration of decanethiol is added in preparation, the bilayer-coated AuNPs exhibit further enhanced stability to cyanide etching, indicating the important role of the alkanethiol in formation of the bilayer. When hydrophilic thiols such as 2-mercaptoethanol and 2-mercaptoethanesulfonate are used in preparation of the bilayer-coated AuNPs, the resulting AuNPs are vulnerable to cyanide etching, reaffirming the role of alkanethiol in anchoring phospholipids to form bilayer.

AuNPs with alkanethiol-anchored bilayers are used as a sensor for membrane binding events utilizing the LSPR sensitivity of AuNPs. Messersmith et al. demonstrated that the homogenous membrane curvature allows more accuracy in measurements of the changes in local refractive index (RI) near surface of AuNPs.[77] HLNCs are prepared using either decanethiol or propanethiol to anchor phospholipids around the AuNP core. The propanethiol hybrid is found to be more sensitive to the LSPR of RI near surface than the decanethiol hybrid, when the interactions between human C-reactive protein and HLNCs are monitored. The initial binding of the protein to the bilayer membrane, the rearrangement of membrane followed by clustering of AuNP cores, and the EDTA-induced release of protein from membrane are the examples of observable events in the LSPR study.

The ability of this HLNC to sense membrane binding events is also applied to study other proteins such as synaptotagmin-7 (Syt7).[78] Syt is a type of protein that promotes exocytosis in neuronal and endocrine cells by binding its C2 domains (C2A and C2B) to membranes in response to an increase in Ca^{2+} concentrations. Using AuNPs with propanethiol-anchored PC/PS phospholipids, Syt7 C2A-induced clustering is detected at low concentrations of Syt7 C2A (≤10 nM) where concentration-induced aggregation is limited. In conjunction with inter-liposomal Förster resonance energy transfer (FRET) assay using liposomes containing either donor fluorophore (NBD) or acceptor fluorophore (RHO), highly sensitive detections of Syt7 C2A membrane binding, protein-induced membrane apposition, and clustering of HLNCs and liposomes are achieved. Binding of Syt7 C2A is observed at concentrations less than 2 μM Ca^{2+}, membrane apposition is detected at 3 μM Ca^{2+}, and clustering is monitored beyond 10 μM Ca^{2+}. Notably, the presence of the lipid bilayer-coated AuNPs greatly enhances the FRET emission ratio between the fluorophore labelled liposomes. The proposed reasoning for the enhancement of FRET emission ratio is the nanoparticle enhanced energy transfer (NEET) when AuNPs are in the vicinity of FRET donor and acceptor pairs such the NBD and RHO.

6.3 Biomimetic HDL

Of great interests are the lipid bilayer-coated nanoparticles developed by Thaxton et al., designed to mimic the size, surface composition, and certain functions of naturally occurring HDL.[79] Centered around the affinity of HDL for cholesterol, a variety of applications for the biomimetic HDL have been demonstrated including protection against atherosclerosis via reverse cholesterol transport, induction of apoptosis in various cancer cells, and transfection of cholesterylated nucleic acids.[80–84]

Naturally occurring HDLs undergo a process called reverse cholesterol transport in which cholesterol is taken up and transported to the liver for excretion. Treatment of atherosclerosis, the accumulation of cholesterol in arterial walls, motivated the initial development of the aforementioned biomimetic HDL HLNC with preserved cholesterol binding capabilities.[79] The original design of the hybrid consists of a AuNP core (~5 nm) capped by disulfide-functionalized lipid PDP PE. The PDP PE lipid monolayer hydrophobically anchors the outer DPPC leaflet which is bound electrostatically by apolipoprotein A1 (apoA1) at the bilayer surface.[85] The biomimetic HDLs prepared in this manner have similar sizes and a comparable number of apolipoproteins and phospholipids to that of naturally occurring HDL. The ability to bind cholesterol is confirmed via binding assays using fluorescent NBD-labelled cholesterol and a dissociation constant (K_d) of 3.8 ± 0.8 is calculated for binding of NBD-cholesterol with the hybrid. To optimize the cholesterol binding and efflux capabilities of this hybrid system, hybrids of various AuNP core sizes (6 or 8 nm) and surface lipid morphologies (bilayer or sulfhydryl-modified DPPC monolayer /with apolipoprotein or without apolipoprotein) are explored.[86] Hybrids with a smaller AuNP core size are found to bind cholesterol stronger than those with larger cores sizes, but at a lower capacity. Hybrids with a bilayer display a higher binding capacity than monolayer DPPC hybrids, but present a weaker binding affinity of cholesterol. The presence of apolipoprotein has no effect on either binding strength or capacity. Ultimately, it is found that the hybrid with a 6 nm AuNP core, a lipid bilayer, and apolipoprotein exhibits the greatest cholesterol efflux capabilities, near doubling that of natural occurring HDL.

Further functionalities can be imparted on the biomimetic HDLs through modification of its lipid. As a proof-of-concept, a nitric oxide (NO) modified lipid DPPNOTE is synthesized and incorporated into the outer leaflet of the biomimetic HDL resulting in dual functions for the hybrid (Fig. 9).[87] The hybrid works in both cholesterol efflux to treat atherosclerosis as well as in NO delivery to treat ischemia through vasodilation.

The cholesterol efflux capabilities of this hybrid have also aided in inducing apoptosis in lymphoma cells.[88] Similar to naturally occurring HDLs, the biomimetic HDLs bind scavenger receptor type B1 (SR-B1), a receptor expressed in many cancer cells, which has a role in facilitating cellular uptake and efflux of cholesterol. The cholesterol-poor nature of the hybrid compared to natural HDL starves the cancer cell of cholesterol, inducing apoptosis. Selective apoptosis of primary chronic lymphocytic leukemia (CLL) is displayed for this biomimetic HDL via the same mechanism of action.[89] Binding of biomimetic HDL to SR-B1 is also demonstrated to generate clustering of the receptors.[90] This clustering inhibits cellular uptake of exosomes, which may play a role in the progression of cancer cells.[90]

Biomimetic HDLs are also used in transfection of cholesterylated nucleic acids to cells that are targeted by HDL.[91–93] The binding of cholesterylated RNA interference (RNAi) to biomimetic HDLs results in protection from nuclease degradation, and transfection into endothelial cells is discovered to silence vascular endothelial growth factor receptor 2 (VEGFR2), inhibiting angiogenesis.[92] An alternative strategy of binding nucleic acids to biomimetic HDLs is to use cationic DOTAP as outer leaflet phospholipid.[93] The positive charge of the lipid allows self-assembly with the nucleic acid as proven with siRNA.

7. Conclusions and future directions

On their own, inorganic nanoparticles and lipid assemblies are readily adaptable systems that can be tailored towards desired properties and functionalities. Naturally, the combination of the two systems into HLNCs offers endless design potentials for biomedical applications. In the last decade or so, the number of studies focused on the development of HLNCs for biomedical purposes have been exponentially increasing and the results have been promising, yet much is left to be explored.

The nanomaterial component of many of these hybrids has been limited to SPIONs, QDs, and most frequently, gold nanostructures that can function in applications including bioimaging, gene therapy, hyperthermia, drug delivery, and cellular labelling due to their unique and exciting optical and/or magnetic properties. However, HLNCs derived from these nanomaterials still provide limited scopes in other important bio-applications. For instance, incorporation of nanomaterials with useful catalytic activity into HLNCs would expand their utilities for potential applications in biocatalysis and bioorthogonal reactions that might allow the development of new bio-transformation and therapeutic strategies in living systems. The availability of catalytic HLNCs that are highly bio-compatible and selective would benefit the ability to conduct highly efficient reactions inside multicellular organisms.

Palladium and platinum are well known for their robust catalytic activity, but have been largely ignored in the HLNC research field. Recently reported properties of palladium nanostructures as prodrug activators lead us to believe that the investigation of HLNCs with catalytic palladium and platinum nanostructures may be a worthwhile endeavour.[94–96] Prodrug activating palladium or platinum nanostructures hybridized with lipid assemblies would allow the highly controlled site-specific drug delivery and the therapeutic use of more potent cytotoxic drugs.[95,96] Alkanethiolate-capped PdNP and PtNP catalysts have been shown to catalyse regio-, chemo-, and stereoselective organic reactions, with the hydrophobic ligand playing a role in directing activity and selectivity.[97–102] Capping the catalytic PdNP and PtNP core with ligands of various functional groups and hybridizing them with lipid assemblies could potentially serve as a model system for enzyme site mimics in addition to above mentioned biocatalysis and bioorthogonal reactions.

Recently, palladium nanostructures as agents for photothermal therapy/anti-microbial/anti-cancer applications have also appeared in the literature. Ultra-thin hexagonal palladium nanosheets with surface plasmon resonance tunable to NIR have been demonstrated to have greater photothermal stability than many gold nanostructures.[103] HLNCs incorporating these palladium-based photothermal agents, therefore, may outperform existing strategies using

AuNPs. PdNPs have also been demonstrated to have antimicrobial and anti-cancer activity, thus targeted-delivery via hybridization with lipid assemblies could be a viable therapeutic option.[104,105]

Many more studies are left to be done in the field of HLNCs. Existing HLNCs can further be optimized for clinical translation and with each novel nanomaterial developed, a new HLNC design with augmented properties can also be proposed. It is evident that HLNCs will play significant roles in biomedicine for years to come.

Acknowledgements

Biographies

Kevin M. Vargas

Kevin Vargas received his B.S. in Biochemistry and B.A. in Chemistry from California State University, Long Beach in 2017. Currently he is pursuing his M.S. in Chemistry at California State University, Long Beach under the supervision of Dr. Young-Seok Shon. His current research is focused on isolating the catalytic influence of surface ligand density and morphology of ligand monolayer in mono-and binary alkanethiolate-capped palladium nanoparticles.

Young-Seok Shon

Young-Seok Shon carried out his doctoral research with T. R. Lee at the University of Houston in Texas, United States, where he received his PhD in 1999. Between 1999 and 2001 he held his postdoctoral position at the University of North Carolina at Chapel Hill (with Royce W. Murray). He began his academic career at Western Kentucky University (2001–2006), before continuing at California State University, Long Beach, where he is currently a professor of Chemistry and Biochemistry. His current main interests are the study and application of colloidal metal nanoparticles and their hybrids.

Abbreviations

DOPC	1,2-Dioleoyl-sn-glycero-3-phosphocholine

|	
DLPC	1,2-dilauroyl-sn -glycero-3-phosphocholine
DPPC	1,2-dipalmitoyl-sn-glycero-3-phosphocholine
DMPC	1,2-dimyristoyl-sn-glycero-3-phosphocholine
DSPC	1,2-distearoyl-sn-glycero-3-phosphocholine
DSPG	1,2-dioctadecanoyl-sn-glycero-3-phospho-(1'-rac-glycerol)
DMPE	1,2-dimyristoyl-sn glycero-3-phosphoethanolamine
DOPG	1,2-dioleoyl-sn-glycero-3-phospho-rac-(1-glycerol)
DOPE	1,2-dioleoyl-sn-glycero-3-phosphoethanolamine
DSPE	1,2-distearoylsn -glycero-3-phosphoethanolamine
DOTAP	1,2-di-(9Z-octadecenoyl)-3-trimethylammonium propane
DOPA	1,2-dioleoyl-sn -glycero-3-phosphate
EPC	hydrogenated L -α -phosphatidylcholine
DPPG	dipalmitoylphosphatidylglycerol
PC	L-α-phosphatidylcholine
HSPC	hydrogenated soy l-α-phosphatidylcholine
Lyso-PPC	1-palmitoyl-2-hydroxy-sn-glycero-3-phosphocholine
DDAB	Didodecyldimethylammonium bromide
DODAB	dimethyldioctadecylammonium bromide
PDP PE	1,2-dipalmitoyl-sn-glycero-3-phosphoethanolamine-N-[3-(2-pyridyldithio)propionate]
DPPTE	1,2-dipalmitoyl-sn -glycero-3- phosphothioethanol
DPPNOTE	1,2-dipalmitoyl-sn -glycero-3 phosphonitrosothioethanol
DSPE-PEG	1,2-distearoyl-sn-glycero- 3-phosphoethanolamine-N-[methoxy(polyethylene glycol)-2000]
MHPC	myristoyl hydroxy phosphatidylcholine
DPPE-PEG	1,2-dipalmitoyl-sn-glycero-3-phosphoethanolamine-N-[methoxy(polyethylene glycol)-2000]
DPPE	1,2-dipalmitoyl-sn-glycero-3-phosphoethanolamine
PS	phosphatidylserine

Notes and references

1. Yang X, Yang M, Pang B, Vara M and Xia Y, Chem. Rev, 2015, 115, 10410–10488. [PubMed: 26293344]

2. Mohammed L, Gomaa HG, Ragab D and Zhu J, Particuology, 2017, 30, 1–14.

3. Rie JV and Thielemans W, Nanoscale, 2017, 9, 8525–8554. [PubMed: 28613299]

4. Yang K, Feng L, Shi X and Liu Z, Chem. Soc. Rev, 2013, 42, 530–547. [PubMed: 23059655]

5. Alarcon EI, Vulesevic B, Argawal A, Ross A, Bejjani P, Podrebara J, Ravichandran R, Phopase J, Suuronen EJ and Griffith M, Nanoscale, 2016, 8, 6484–6489. [PubMed: 26949000]

6. Gavia DJ and Shon Y-S, ChemCatChem, 2015, 7, 892–900. [PubMed: 25937846]

7. Rai M, Ingle AP, Birla S, Yadav A and Santos CA, Crit. Rev. Microbiol, 2016, 42, 696–719. [PubMed: 26089024]

8. Chandra S, Barick KC and Bahadur D, Adv. Drug Deliv. Rev, 2011, 63, 1267–1281. [PubMed: 21729727]

9. He X and Ma N, Colloids Surf, 2014, 124, 118–131.

10. Sapsford KE, Algar WR, Berti L, Gemmill KB, Casey BJ, Oh E, Stewart MH and Medintz IL, Chem. Rev 2013, 115, 1904–2074.

11. Ueno T, Suzuki M, Goto T, Matsumoto T, Nagayama K and Watanabe Y, Angew. Chem. Int. Ed, 2004, 43, 2527–2530.

12. Li PC, Li D, Zhang LX, Li GP and Wang EK, Biomaterials, 2008, 29, 3617–3624. [PubMed: 18571230]

13. Daniel MC and Astruc D, Chem. Rev, 2004, 104, 293–346. [PubMed: 14719978]

14. Katz E and Willner I, Angew. Chem. Int. Ed, 2004, 43, 6042–6108.

15. Medintz I, Uyeda H, Goldman E and Mattoussi H, Nat. Mater, 2005, 4, 435–446. [PubMed: 15928695]

16. Biju V, Itoh T, Anas A, Sujith A and Ishikawa M, Anal. Bioanal. Chem, 2008, 391, 2469–2495. [PubMed: 18548237]

17. Gupta AK, Naregalkar RR, Vaidya VD and Gupta M, Nanomedicine, 2007, 2, 23–29. [PubMed: 17716188]

18. Allen TM and Cullis PR, Adv. Drug Deliv. Rev, 2013, 65, 36–48. [PubMed: 23036225]

19. Thaxton CS, Rink JS, Naha PC and Cormode DP, Adv. Drug Deliv. Rev, 2016, 106, 116–131. [PubMed: 27133387]

20. Kalaycioglu GD and Aydogan N, Colloids Surf. A, 2016, 510, 77–86.

21. James ND, Coker RJ, Tomlinson D, Harris JR, Gompels M, Pinching AJ and Stewart JS, Clin. Oncol. (R. Coll. Radiol.), 1994, 6, 294–296. [PubMed: 7530036]

22. Haluska CK, Riske KA, Marchi-Artzner C, Lehn J-M, Lipowsky R and Dimova R, Proc. Natl. Acad. Sci. U.S.A, 2006, 103, 15841–15846. [PubMed: 17043227]

23. Lei G and MacDonald RC, Biophys. J, 2003, 85, 1585–1599. [PubMed: 12944275]

24. Marrink SJ and Mark AE, J. Am. Chem. Soc, 2003, 125, 11144–11145. [PubMed: 16220905]

25. Prausnitz MR and Langer R, Nat. Biotechnol, 2008, 26, 1261–1268. [PubMed: 18997767]

26. Sinico C and Fadda AM, Expert Opin. Drug Deliv, 2009, 6, 813–825. [PubMed: 19569979]

27. Zhang L and Granick S, Nano Lett, 2006, 6, 813–825.

28. Moghimi SM and Szebeni J, Pro. Lipid. Res, 2003, 42, 463–478.

29. Zhang L, Dammann K, Bae SC and Granick S, Soft Matter, 2007, 3, 551–553.

30. Pornpattananangkul D, Zhang L, Aryal S, Obonyo M, Vecchio K, Huang C-M and Zhang L, J. Am. Chem. Soc, 2011, 133, 4132–4139. [PubMed: 21344925]

31. Pornpattananangkul D, Olson S, Aryal S, Sartor M, Huang C-M, Vecchio K, and Zhang L, ACS Nano, 2010, 4, 1935–1942. [PubMed: 20235571]

32. Thamphiwatana S, Fu V, Zhu J, Lu D, Gao W and Zhang L, Langmuir, 2013, 29, 12228–12233. [PubMed: 23987129]

33. Wang B, Zhang L, Bae SC and Granick S, Proc. Natl. Acad. Sci. U.S.A, 2008, 105, 18171–18175. [PubMed: 19011086]

34. Wang F, Curry DE and Liu H, Langmuir, 2015, 31, 13271–13274. [PubMed: 26595673]

35. Bhat A, Edwards LW, Fu Z, Badman DL, Huo S, Jin AJ and Lu Q, Appl. Phys. Lett, 2016, 109, 263106 [PubMed: 28104921]

36. Wang F and Liu J, Nanoscale, 2015, 7, 15599–15604 [PubMed: 26372064]

37. Liu Y and Liu J, Langmuir, 2016, 32, 13276–13283. [PubMed: 27951710]

38. Thamphiwatana S, Gao W, Pornpattananangkul D, Zhang Q, Fu V, Li J, Li J, Obonyo M and Zhang L, J. Mater. Chem. B, 2014, 2, 8201–8207. [PubMed: 25544886]

39. Troutman TS, Barton JK and Romanowski M, Adv. Mater, 2008, 20, 2604–2608. [PubMed: 21494416]

40. Rengan AK, Jagtap M, De A, Banerjee R and Srivastava R, Nanoscale, 2014, 6, 916–923. [PubMed: 24281647]

41. Abbasi A, Park K, Bose A and Bothun GD, Langmuir, 2017, 33, 5321–5327. [PubMed: 28486807]

42. Rengan AK, Bukhari AB, Pradhan A, Malhotra R, Banerjee R, Srivastava R and De A, Nano Lett, 2015, 15, 842–848. [PubMed: 25554860]

43. Bhuvana M and Dharuman V, Sens. Actuators B Chem, 2016, 223, 157–165.

44. Bhuvana M and Dharuman V, Analyst, 2014, 139, 2467. [PubMed: 24652193]

45. Park S-H, Oh S-G, Mun J-Y and Han S-S, Colloids Surf. B, 2005, 44, 117–122.

46. Park S-H, Oh S-G, Mun J-Y and Han S-S, Colloids Surf. B, 2006, 48, 112–118.

47. Bothun GD, J. Nanobiotech, 2008, 6, 13.

48. Chen Y, Bose A and Bothun GD, ACS Nano, 2010, 4, 3215–3221. [PubMed: 20507153]

49. Preiss MR, Hart A, Kitchens C and Bothun GD, J. Phys. Chem. B, 2017, 121, 5040–5047. [PubMed: 28441023]

50. Rasch MR, Rossinyol E, Hueso JL, Goodfellow BW, Arbiol J and Korgel BA, Nano Lett, 2010, 10, 3733–3739. [PubMed: 20731366]

51. White II GV, Chen Y, Roder-Hanna J, Bothun GD and Kitchens CL, ACS Nano, 2012, 6, 4678–4685. [PubMed: 22632177]

52. Malekar SA, Sarode AL, BachII AC, Bose A, Bothun G and Worthen DR, AAPS PharmSciTech, 2015, 16, 1335–1343. [PubMed: 25899799]

53. Amstad E, Kohlbrecher J, Müller E, Schweizer T, Textor M and Reimhult E, Nano Lett, 2011, 11, 1664–1670. [PubMed: 21351741]

54. Bao Q-Y, Zhang N, Geng D-D, Xue J-W, Merritt M, Zhang C and Ding Y, Int. J. Pharm, 2014, 477, 408–415. [PubMed: 25455782]

55. Zhang N, Chen H, Liu A-Y, Shen J-J, Shah V, Zhang C, Hong J and Ding Y, Biomaterials, 2016, 74, 280–291. [PubMed: 26461120]

56. Kautzka Z, Clement S, Goldys EM and Deng W, Int. J. Nanomedicine, 2017, 12, 969–977. [PubMed: 28203076]

57. Gopalakrishnan G, Danelon C, Izewska P, Prummer M, Bolinger P-Y, Geissbühler I, Demurtas D, Dubochet J and Vogel H, Angew. Chem. Int. Ed, 2006, 45, 5478–5483.

58. Genç R, Clergeaud G, Ortiz M and O'Sullivan CK, Langmuir, 2011, 27, 10894–10900. [PubMed: 21786795]

59. Clergeaud G, Genç R, Ortiz M and O'Sullivan CK, Langmuir, 2013, 29, 15405–15413. [PubMed: 24246054]

60. Lee J-H, Shin Y, Lee W, Whang K, Kim D, Lee LP, Choi J-W and Kang T, Sci. Adv, 2016, 2, 1–9.

61. Viitala L, Pajari S, Lajunen T, Kontturi L-S, Laaksonen T, Kuosmanen P, Viitala T, Urtti A and Murtomäki L, Langmuir, 2016, 32, 4554–4563. [PubMed: 27089512]

62. Lajunen T, Viitala L, Kontturi L-S, Laaksonen T, Liang H, Vuorimaa-Laukkanen E, Viitala T, Guével XL, Yliperttula M, Murtomäki L and Urtti A, J. Control. Release, 2015, 203, 85–98. [PubMed: 25701610]

63. Tai L-A, Tsai P-J, Wang T-C, Wang Y-J, Lo L-W and Yang C-S, Nanotechnology, 2009, 20, 135101. [PubMed: 19420485]

64. Chuang ST, Shon Y-S and Narayanaswami V, Int. J. Nanomedicine, 2017, 12, 8495–8510. [PubMed: 29225464]

65. Allijn IE, Leong W, Tang J, Gianella A, Mieszawska AJ, Fay F, Ma G, Russell S, Callo CB, Gordon RE, Korkmaz E, Post JA, Zhao Y, Gerritsen HC, Thran A, Proksa R, Daerr H, Storm G, Fuster V, Fisher EA, Fayad ZA, Mulder WJM and Cormode DP, ACS Nano, 2013, 7, 9761–9770. [PubMed: 24127782]

66. Edris B, Weiskopf K, Volkmer AK, Volkmer JP, Willingham SB, Conteras-Trujillo H, Liu J, Majeti R, West RB, Fletcher JA, Beck AH, Weissman IL, Van de Rijin M, Proc. Natl. Acad. Sci. U.S.A, 2012, 109, 6656–6661. [PubMed: 22451919]

67. Grillone A, Riva ER, Mondini A, Forte C, Calucci L, Innocenti C, de Julian Fernandez C, Cappello V, Gemmi M, Moscato S, Ronca F, Sacco R, Mattoli V and Ciofani G, Adv. Healthc. Mater, 2015, 4, 1681–1690. [PubMed: 26039933]

68. Calucci L, Agostina G, Riva ER, Mattoli V, Ciofani C and Forte C, J. Phys. Chem. C, 2017, 121, 823–829.

69. Lim YT, Noh Y-W, Cho J-H, Han JH, Choi BS, Kwon J, Hong KS, Gokarna A, Cho Y-H and Chung BH, J. Am. Chem. Soc, 2009, 131, 17145–17154. [PubMed: 19894710]

70. Lim YT, Cho MY, Kang J-H, Noh Y-W, Cho J-H, Hong KS, Chung JW and Chung BH, Biomaterials, 2010, 31, 4964–4971. [PubMed: 20346494]

71. Bae PK and Chung BH, Nano Converg, 2014, 1, 23. [PubMed: 28191403]

72. Zhang L, Sun X, Song Y, Jiang X, Dong S and Wang E, Langmuir, 2006, 22, 2838–2843. [PubMed: 16519492]

73. Li P, Zhang L, Ai K, Li D, Liu X and Wang E, J. Control. Release, 2008, 129, 128–134. [PubMed: 18508147]

74. Li P, Li D, Zhang L, Li G and Wang E, Biomaterials, 2008, 29, 3617–3624. [PubMed: 18571230]

75. Li D, Li G, Li P, Zhang L, Liu Z, Wang J and Wang E, Biomaterials, 2010, 31, 1850–1857. [PubMed: 19945155]

76. Sitaula S, Mackiewicz MR, and Reed SM, Chem. Commun, 2008, 3013–3015.

77. Messersmith RE, Nusz GJ and Reed SM, J. Phys. Chem. C, 2013, 117, 26725–26733.

78. Hamilton DJ, Coffman MD, Knight JD and Reed SM, Langmuir, 2017, 33, 9222–9230. [PubMed: 28850236]

79. Thaxton CS, Daniel WL, Giljohann DA, Thomas AD and Mirkin CA, J. Am. Chem. Soc, 2009, 131, 1384–1385. [PubMed: 19133723]

80. Damiano MG, Mutharasan RK, Tripathy S, McMahon KM and Thaxton CS, Adv. Drug Deliv. Rev, 2013, 65, 649–662. [PubMed: 22921597]

81. McMahon KM and Thaxton CS, Expert Opin. Drug Deliv, 2014, 11, 231–247. [PubMed: 24313310]

82. Foit L, Giles FJ, Gordon LI and Thaxton CS, Expert Rev. Anticancer Ther, 2015, 15, 27–34. [PubMed: 25487833]

83. Mutharasan RK, Foit LF and Thaxton CS, J. Mater. Chem. B Mater. Biol. Med, 2016, 4, 188–197. [PubMed: 27069624]

84. Thaxton CS, Rink JS, Naha PC and Cormode DP, Adv. Drug Deliv. Rev, 2016, 106, 116–131. [PubMed: 27133387]

85. Lai C-T, Sun W, Palekar RU, Thaxton CS and Schartz GC, ACS Appl. Mater. Interfaces, 2017, 9, 1247–1254. [PubMed: 28001031]

86. Luthi AJ, Zhang H, Kim D, Gijohann DA, Mirkin CA and Thaxton CS, ACS Nano, 2012, 6, 276–285. [PubMed: 22117189]

87. Rink JS, Sun W, Misener S, Wang J-J, Zhang ZJ, Kibbe MR, Dravid VP, Venkatraman S and Thaxton CS, ACS Appl. Mater. Interfaces, 2018, 10, 6904–6916. [PubMed: 29385802]

88. Yang S, Damiano MG, Zhang H, Tripathy S, Luthi AJ, Rink JS, Ugolkov AV, Singh ATK, Dave SS, Gordon LI and S Thaxton C, Proc. Natl. Acad. Sci. U.S.A, 2013, 110, 2511–2516. [PubMed: 23345442]

89. McMahon KM, Scielzo C, Angeloni NL, Deiss-Yehiely E, Scarfo L, Ranghetti P, Ma S, Kaplan J, Barbaglio F, Gordon LI, Giles FJ, Thaxton CS, Ghia P, Oncotarget, 2017, 8, 11219–11227. [PubMed: 28061439]

90. Plebanek MP, Mutharasan RK, Volpert O, Matov A, Gatlin JC and Thaxton CS, Sci. Rep, 2015, 5, 15724. [PubMed: 26511855]

91. McMahon KM, Mutharasan RK, Tripathy S, Veliceasa D, Bobeica M, Shumaker DK, Luthi AJ, Helfand BT, Ardehali H, Mirkin CA, Volpert O, and Thaxton CS, Nano Lett, 2011, 11, 1208–1214. [PubMed: 21319839]

92. Tripathy S, Vinokour E, McMahon KM, Volpert OV and Thaxton CS, Part. Part. Syst. Charact, 2014, 31, 1141–1150. [PubMed: 25400330]

93. McMahon KM, Plebanek MP and Thaxton CS, Adv. Funct. Mater 2016, 26, 7824–7835. [PubMed: 28717350]

94. Dumas A and Couvreur P, Chem. Sci, 2015, 6, 2153–2157. [PubMed: 28694948]

95. Weiss JT, Dawson JC, Macleod KG, Rybski W, Fraser C, Torres-Sanchez C, Patton EE, Bradley M, Carragher NO and Unciti-Broceta A, Nat. Commun, 2014, 5, 3277. [PubMed: 24522696]

96. Balbin A, Gaballo F, Ceballos-Torres J, Prashar S, Fajardo M, Kaluderovic GN and Gomez-Ruiz S, RSC Adv, 2014, 4, 54775–54787.

97. Chen T-A and Shon Y-S, Catalysts, 2018, 8, 428.

98. San KA and Shon Y-S, Nanomaterials, 2018, 8, 346.

99. Chen T-A and Shon Y-S, Catal. Sci. Technol, 2017, 7, 4823–4829. [PubMed: 29713450]

100. Maung MS and Shon Y-S, J. Phys. Chem. C, 2017, 121, 20882–20891.

101. San KA, Chen V and Shon Y-S, ACS Appl. Mater. Interfaces, 2017, 9, 9823–9832. [PubMed: 28252941]

102. Zhu JS and Shon Y-S, Nanoscale, 2015, 7, 17786–17790. [PubMed: 26455381]

103. Weiss JT, Dawson JC, Fraser C, Rybski W, Torres-Sanchez C, Bradley M, Patton EE, Carragher NO and Unciti-Broceta A, J. Med. Chem, 2014, 57, 5395–5404. [PubMed: 24867590]

104. Huang XQ, Tang SH, Mu XL, Dai Y, Chen GX, Zhou ZY, Ruan FX, Yang ZL and Zheng NF, Nat. Nanotechnol, 2011, 6, 28–32. [PubMed: 21131956]

105. Adams CP, Walker KA, Obare SO and Docherty KM, PLoS One, 2014, 9, e85981. [PubMed: 24465824]
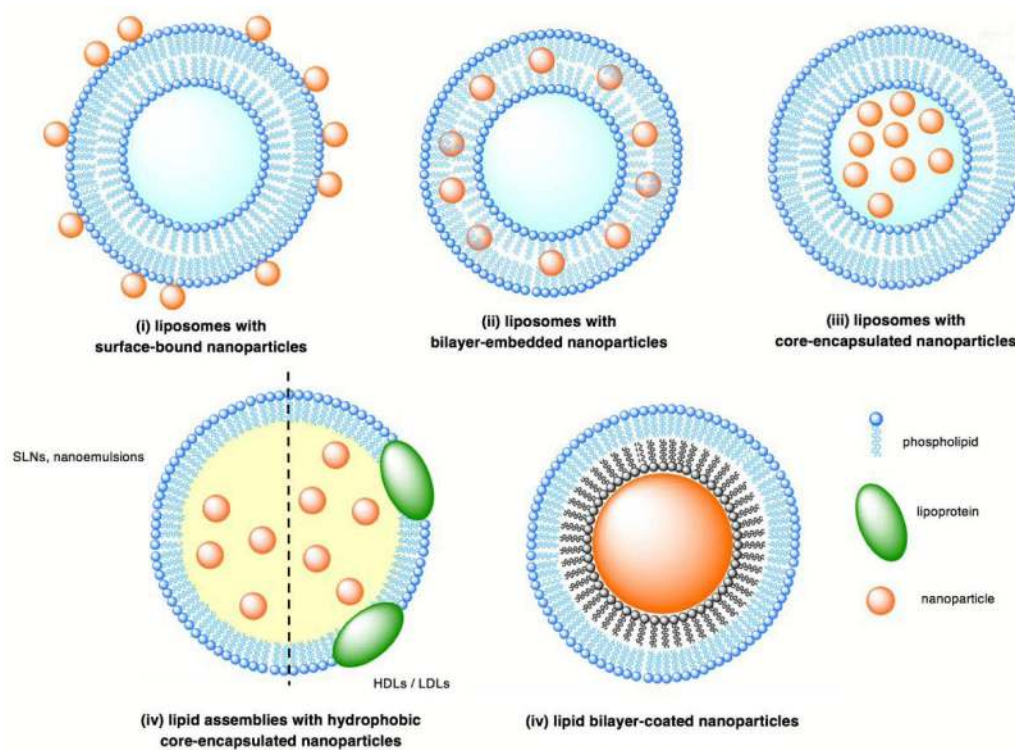
Fig. 1.
Illustration of the five classes of HLNCs: (i) liposomes with surface-bound nanoparticles, (ii) liposomes with bilayer-embedded nanoparticles, (iii) liposomes with core-encapsulated nanoparticles, (iv) lipid assemblies with hydrophobic-core encapsulated nanoparticles, and (v) lipid bilayer-coated nanoparticles.
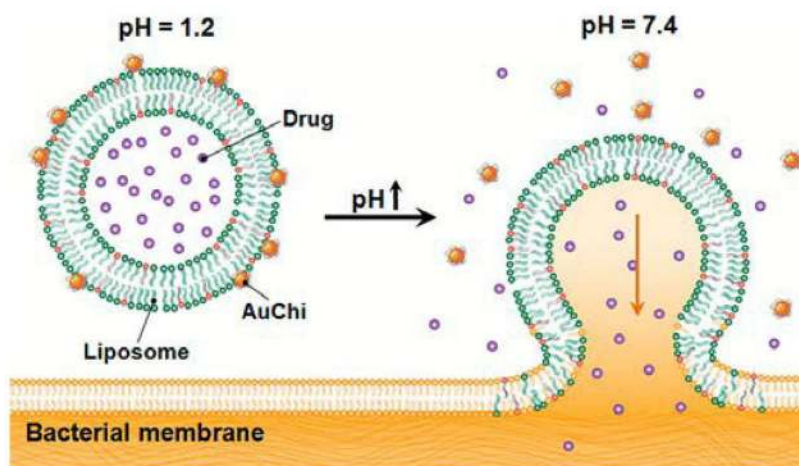
Fig 2.
Schematic illustration of a phospholipid liposome stabilized by chitosan-modified gold nanoparticles (AuChi-liposome) for pH responsive gastric drug delivery. At gastric pH (pH = 1.2), the liposome is stabilized by binding of protonated AuChi nanoparticles. At physiological condition (pH = 7.4), AuChi nanoparticles are deprotonated and thus detach from the liposome, resulting in bare liposome with restored fusion and drug release properties. Reproduced with permission from ref. 32. Copyright © 2013, American Chemical Society.
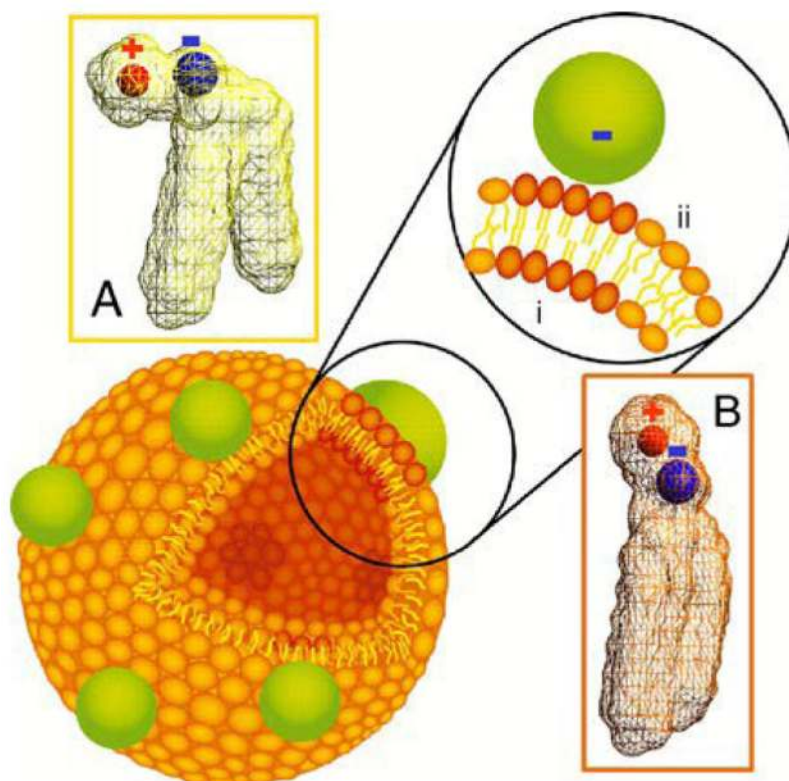
Fig. 3.
Schematic diagram of a phospholipid bilayer vesicle with bound nanoparticles. Binding of anionic nanoparticles to a lipid bilayer in the fluid phase causes the nanoparticle to template a gel phase in the place where the nanoparticle binds. Binding-induced reorientation of the phosphocholine (PC) head group causes lipids in the fluid phase to have lower density (A) than in the gel phase (B). In the PC head group, P and N are denoted by blue and red, respectively. Reproduced with permission from ref. 33. Copyright © 2008, National Academy of Sciences
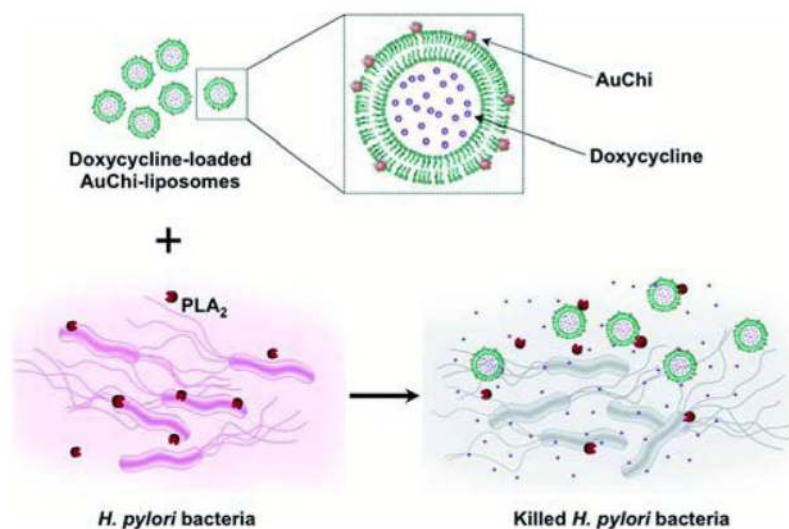
Fig. 4.
Schematic illustration of phospholipase A2 (PLA2)-triggered antibiotic release from liposomes stabilized by chitosan-modified gold nanoparticles (AuChiliposome) to treat bacteria (e.g., H. pylori) that secrete the enzyme. Antibiotic (e.g. doxycycline)-loaded liposomes are prohibited from fusion by adsorbing AuChi nanoparticles onto their surface. Once the AuChi-liposomes encounter bacteria-secreted PLA2, the enzyme cleaves the phospholipids that form the liposome membranes and thus releases the encapsulated antibiotics, which subsequently kill or inhibit the growth of the bacteria. Reproduced with permission from ref. 38. Copyright © 2014, The Royal Society of Chemistry.
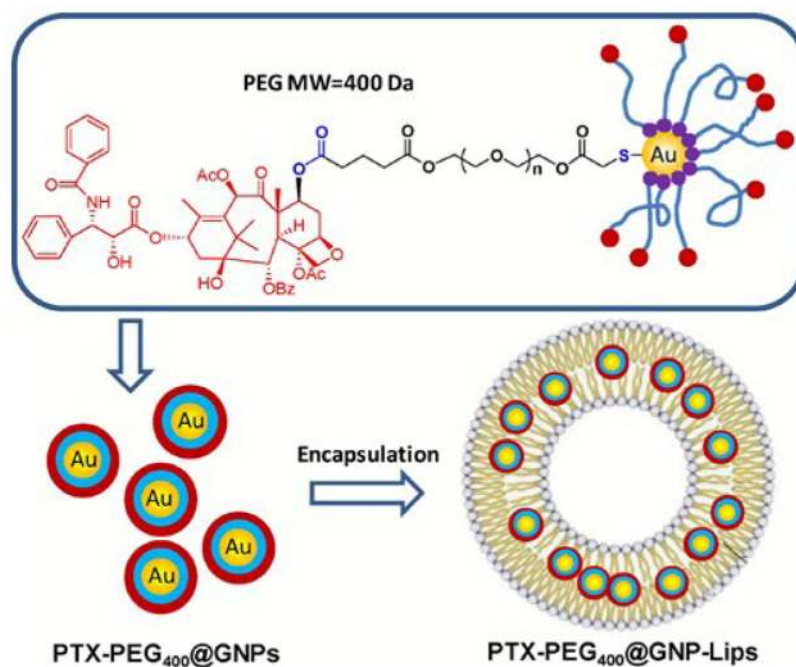
Fig. 5.
The chemical structure of PTX-conjugated GNPs (PTX-PEG$_{400}$@GNPs) and composition illustration of their encapsulated liposomes (PTX-PEG$_{400}$@GNP-Lips). Reproduced with permission from ref. 54. Copyright © 2014, Elsevier Ltd.
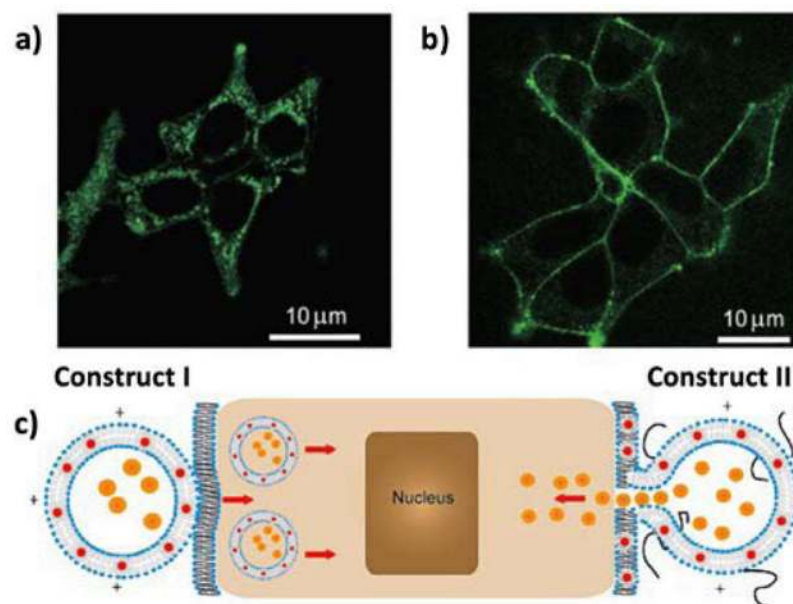
Fig. 6.
Interaction of HVs with HEK293 cells. a,b) Confocal micrographs of HEK293 cells 30 s after addition of vesicles: a) construct I vesicles are totally internalized into the cells; b) construct II vesicles selectively labelled the cell membrane without internalization into the cytoplasm. c) Cartoon illustrating interactions of construct I and II HVs with living cells. Orange dots in the interior of the HVs represent any deliverable water-soluble molecules. Reproduced with permission from ref. 57. Copyright © 2006, Wiley-VCH Verlag GmbH & Co. KGaA, Weinheim.
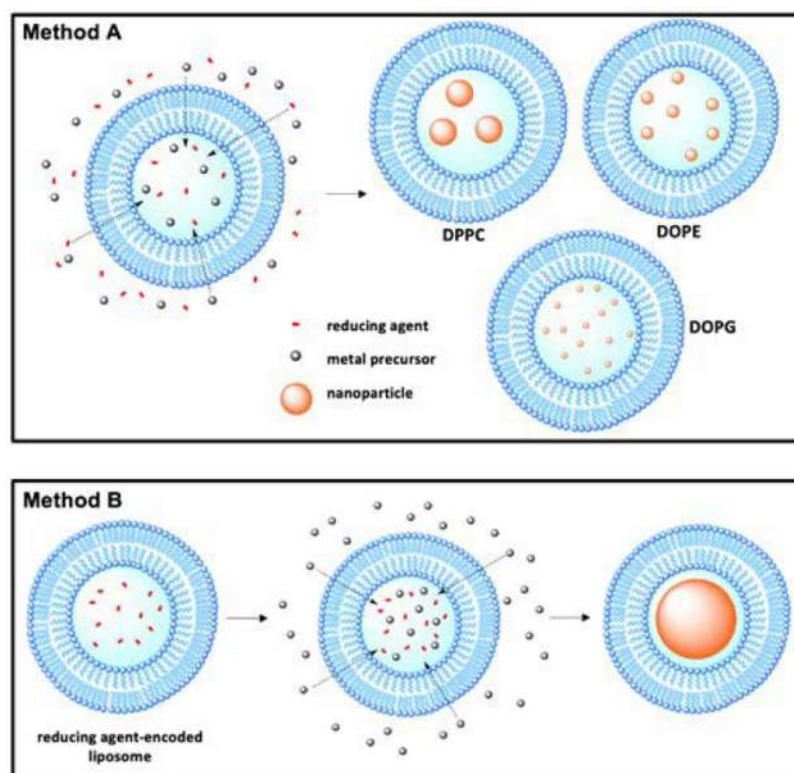
Fig. 7.
Schematic illustration of the methods of nanoparticle synthesis within liposomal core. Method A represents the nanoparticle synthesis utilized in ref. 58 and 59. Method B the reducing agent-encoded liposome method of nanoparticle synthesis utilized ref. 60.
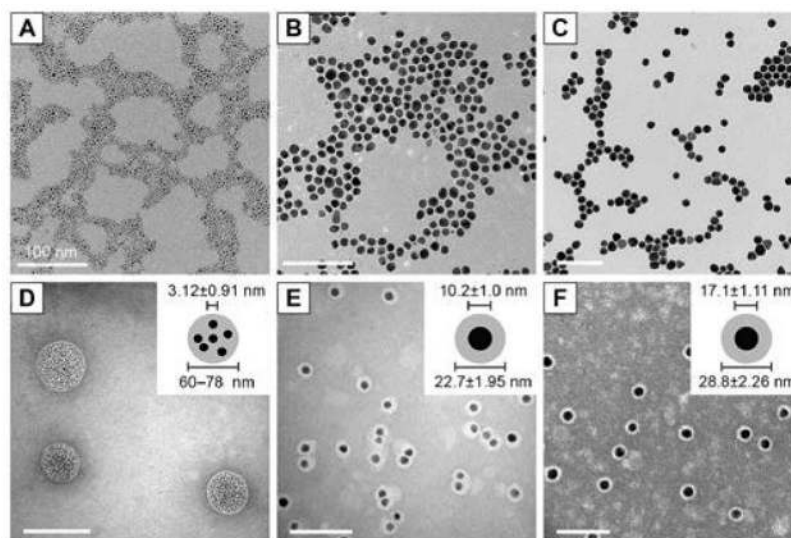
Fig. 8.
TEM images and histograms of core AuNP and rHDL-AuNP. TEM images of core (A–C) and rHDL-AuNP (D–F) are shown for 3 nm (A, D), 10 nm (B, E), and 17 nm (C, F) AuNP. The rHDL-AuNP samples were negatively stained with 2% uranyl acetate. All scale bars represent 100 nm. Insets in (Panels D–F) show schematic representation of AuNP core and lipoprotein shell that was measured. Reproduced with permission from ref. 64. Copyright © 2017, Dove Medical Press Limited.
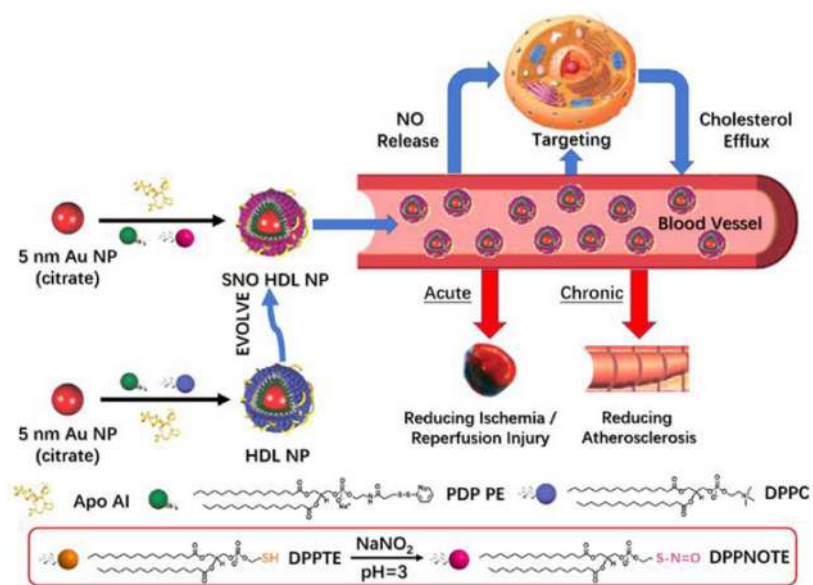
Fig. 9.
Preparation, properties, and functions of SNO HDL NPs. Reproduced with permission from ref. 87. Copyright © 2018, American Chemical Society.

Table 1.

Summary of HLNC components, assembly methods, and biomedical applications

Nanoparticle component	Lipid component	Assembly methods	Biomedical applications	Ref.
Type (i) HLNC				
PS nanoparticle (20 nm)	DLPC	cosonication of liposome/NP	fusion stabilization of liposomes	27,29
chitosan-AuNP (10 nm)	EPC, cholesterol	cosonication of liposome/NP	bacterial toxin-triggered drug release	30
MPA-AuNP(4nm)	EPC, DOTAP	cosonication of liposome/NP	pH-triggered drug release	31
chitosan-AuNP (10 nm)	EPC, DOPA	cosonication of liposome/NP	pH-triggered drug release	32
chitosan-AuNP (10 nm)	DSPC, DSPG	cosonication of liposome/NP	enzyme-triggered drug release	38
Au nanoshell	DSPC, cholesterol	precursor reduction on liposomal surface	NIR-triggered drug release/ PTT, multimodal imaging	40,42
Au nanoshell	DOPC, DOPG	layersome direct reduction/seeded growth method	NIR-triggered drug release/ PTT, multimodal imaging	41
citrate-AuNP (~5 nm)	DOTAP	cosonication of liposome/NP	DNA transfection	43,44
Type (ii) HLNC				
oleic acid-capped SPION (5 nm)	DPPC	thin film hydration w/ NP	AMF-triggered drug release	48,52
palmityl-nitroDOPA-capped SPION (<5.5nm)	DSPC	thin film hydration w/ NP	AMF-triggered drug release	53
PTX-PEG400-AuNP (~3.4 nm)	PC, cholesterol	thin film hydration w/ NP	anticancer (PTX delivery)	54,55
dodecanethiol-AuNP (3–5 nm)	HSPC	thin film hydration w/ NP, extrusion	NP-enhanced photodynamic therapy	56
MIDDLEO-capped QD (5 nm)	DM PC, DOTAP	swelling/electroswelling	controlled cellular imaging	57
Type (iii) HLNC				
AuNP(2–8nm)	DOPG, lyso-PC	curvature-tuned preparation	liposomal nanoreactor	58
PdNP(~2, 9,16 nm)	DOPG, DOPE, DPPC	curvature-tuned preparation	liposomal nanoreactor	59
Au-, Ag-, Pd-, Pt-, Au/Pt-Au/Pd-, Au/Ag-NP (~30–160 nm)	DSPC	thin film hydration with reducing agent solution, extrusion	liposomal nanoreactor	60
Au nanorod (41 nm length)	DPPC	thin film hydration w/ NP, extrusion	NIR-triggered drug release	61
Au nanorod/nanostar	DPPC, DSPC, lyso-PC, DSPE-PEG	reverse-phase evaporation	visible/NIR-triggered drug release	62
SPION (3–5 nm)	DPPC, DSPC	thin film hydration w/ NP, extrusion	AMF-triggered drug release	63
Type (iv) HLNC				
tetradecanethiol-AuNP (3,10,17 nm)	DMPC	thin film, NP, apoE3 cosonication	tumor-targeting, PTT	64
dodecanethiol-AuNP (2–3 nm)	MHPC, DMPE	lipid coated NP cosonicated w/ LDL	Tumor-targeting, biolabelling	65
SPION	cetyl palmitate	oil-in-water homogenization	Magnetically-directed drug delivery	67

Nanoparticle component	Lipid component	Assembly methods	Biomedical applications	Ref.
SPION (10 nm)	cetyl palmitate	oil-in-water homogenization	MRI contrast agents	68
PFC-capped QD (3–5 nm)	EPC, DPPE-PEG	ligand-exchange, PFC emulsification	^{19}F-MR/optical imaging	69,70
PFC-capped QD	EPC, DSPE-PEG-NHS	ligand-exchange, PFC emulsification	tumor-targeting, ^{19}F-MR/optical imaging	71
Type (v) HLNC				
DDAB/DODAB-capped AuNP (7–18 nm)	DPPC, DDAB, DOTAP	precursor reduction in lipid solution	DNA transfection	72–75
alkanethiol-AuNP (~20, 40 nm)	PC, PS, DPPE-NBD, DPPE-RHO	alkanethiol ligand exchange in lipid solution	monitor membrane binding events	77,78
PDP PE-capped AuNP	DPPC, PDP PE	PDP PE ligand exchange in solution with outer lipid and apolipoprotein	atherosclerosis treatment, induction cancer cell apoptosis, inhibit angiogenesis, nucleic acid transfection	79–84, 88–92
PDP PE-capped AuNP	DPPNOTE, PDP PE	PDP PE ligand exchange in solution with outer lipid and apolipoprotein	atherosclerosis treatment, induced vasodilation	87
PDP PE-capped AuNP	DOTAP, DOPC, PDP PE	PDP PE ligand exchange in solution with outer lipid and apolipoprotein	Nucleic acid transfection	93